NASA-CR-194593

EVAPORATION FROM A MENISCUS WITHIN A CAPILLARY TUBE IN MICROGRAVITY

Yearly Report
1 December 1992 - 30 November 1993

November 3, 1993

Grant No. NAG3-1391

University of Dayton
Mechanical and Aerospace Engineering
Dayton, Ohio 45469

YEARLY - NAG3-1391

EVAPORATION FROM A CAPILLARY MENISCUS IN MICROGRAVITY

10-30-93

by

Dr. K. P. Hallinan

University of Dayton

The following represents a summary of progress made on the project "Evaporation from a Capillary Meniscus in Microgravity" being conducted at the University of Dayton during the period 12-1-92 through 11-30-93. The efforts during this first year of the grant have focused upon the following specific tasks: (i). Application of a 3-D scattering particle image velocimetry technique to thin film velocity field measurement; (ii) Modelling the thermo-fluid behavior of the evaporating meniscus in 0-g within large diameter capillaries; (iii) Conceptualization of the space flight test cell (loop) configuration; (iv) Construction of prototypes of the test loop configuration; (v) Conduct of experiments in 0-g in the 2.2 second drop tower at NASA-LeRC to study evaporation from a capillary mensiscus within a square cuvette; and (vi) Investigation of the effect of vibrations on the stability of the meniscus. An overview of the work completed within these six task areas follows. Also, included is a listing of the students working in each of these focus areas.

3-D Particle Image Velocimetry

A great deal of effort has been directed toward the application of the 3-D scattering particle image velocimetry technique, developed by B. Ovryn of Sverdrup, toward the measurement of the velocity field within the evaporating thin film of liquid adjoining the bulk meniscus, as it is this technique, more than anything else, which is vital for insuring the success of the future space flight experiment. Efforts have focused chiefly on: the optimization of the light source (both coherent laser and Koehler illumination have been tried); the determination of the effect of decreasing seeding particle size upon the sensitivity of the technique in measuring particle location relative to an imaging plane and, as well, velocities normal to the imaging plane; and upon the determination of the effect of particle shape on the effectiveness of the technique. Additionally, a significant amount of time has addressed the choice of particles to be seeded in the working fluids which are being considered in the future flight experiemnts (pentane, F-113, ammonia).

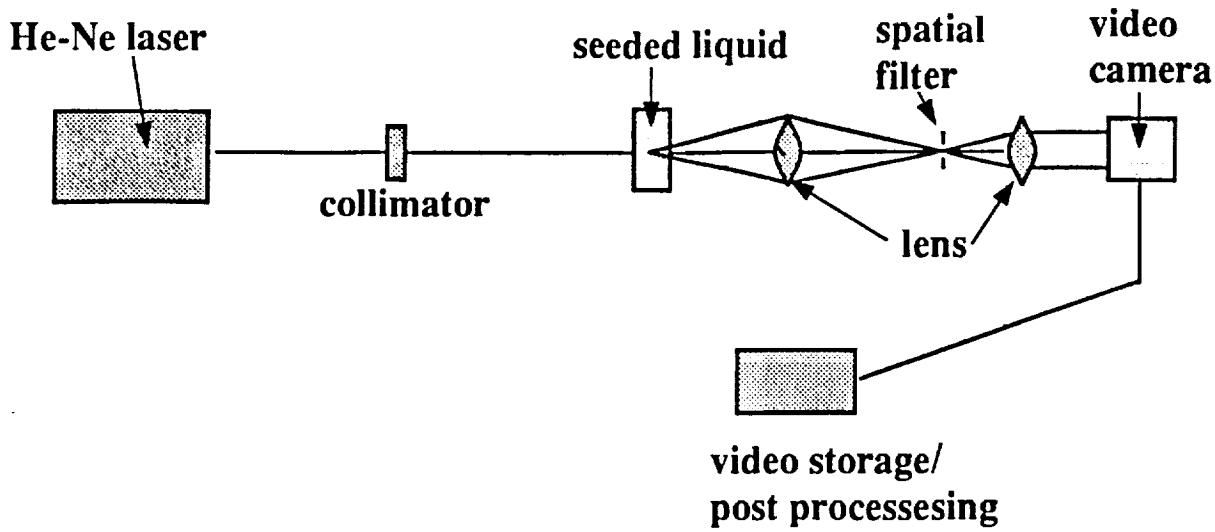

Figure 1: Schematic of P.I.V. optics with laser illumination

The basic idea of the technique is to transmit a coherent or partially coherent light source through a seeded volume of fluid. The resulting forward scattered diffraction pattern is imaged through a video microscope connected to a CCD camera. The diffraction pattern changes as the distance from the particle to the image plane changes. If a particle is viewed in focus, an image is observed. However, if the particle moves out of focus, a diffraction pattern will be observed. At the center of the diffraction pattern is a bright region called Poisson's spot. The center of the Poisson's spot is coincident with the center of the particle. Furthermore, the size of Poisson's spot varies as a particle moves paraxially.

Work is on-going toward the optimization of the lighting source for the technique. With regard to particle size, although it would be ideal to use particles in the sub-micron range, preliminary results indicate that best results can be practically realized if the particle size is maximized. However, given a maximum film thickness of no more than 100 μm of interest in the future space flight experiment, particle sizes no bigger than 5 μm can be considered without the particles disturbing the flow significantly. Thus, all efforts are now concentrated upon optimizing lighting, imaging magnification, and image processing with particles of this size. Finally, the choice of particles will depend upon the working fluid, but candidate particles have been acquired for future testing with each of the working fluids considered. This testing will follow further development of the technique.

Figure 1 represents a schematic of the configuration for the P.I.V. technique using the coherent illumina-

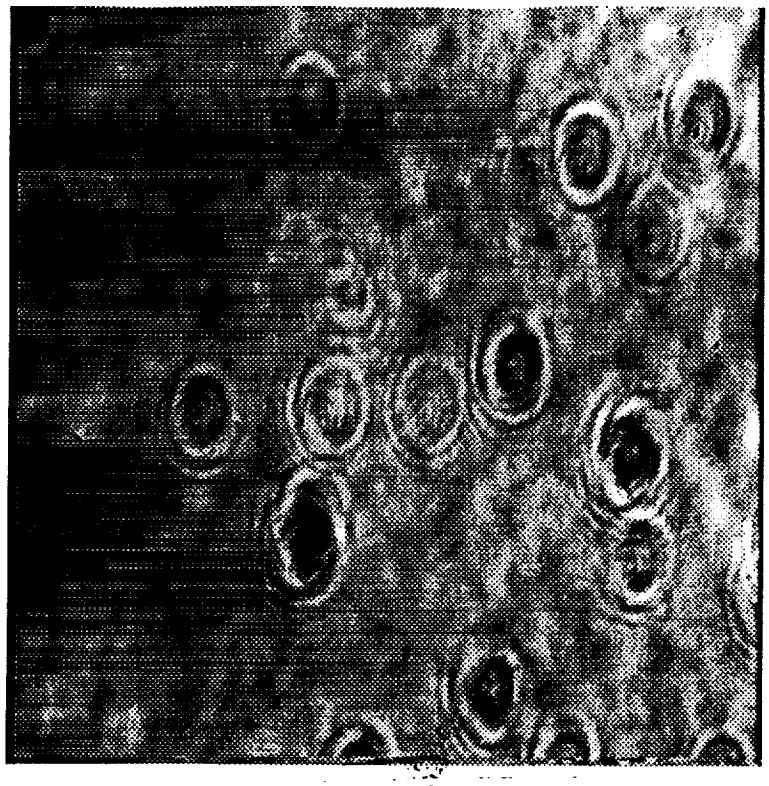

Figure 2: Raw image of diffraction patterns of 5 μm alumina particle in water .

tion from a 35 mW He-Ne laser. Fig.'s 2 and 3 show representative diffraction patterns observed downstream of the 5 micron alumina test particles using laser illumination in two successive frames. Clear from these raw images is that there is appreciable noise due to dust and do to laser speckle. The particles are roughly 50 microns out of focus. The particles/fluid mixture for testing purposes are contained between two optically flat, quartz slides, 1 mm in thickness. This means for containing the particles is strictly being used to optimize the lighting and the imaging optics. It has been determined that a higher resolution camera is essential. Higher magnification for the imaging optics is also deemed necessary.

In addition to fine tuning the imaging technique, work is progressing on the subsequent processesing of the images to enhance the contrast of the diffraction rings. Figure 4 demonstrates how the simple process of subtraction of two successive images can be used to filter out the static noise that may be present in the optical system. Obvious from the figure is that after the subtraction process only those particles which are moving will still be present after the processing. Moreover, additional processing can be performed on the subtracted image shown in Fig. 4 to enhance the contrast of the rings. In Fig. 5 a simple constrast

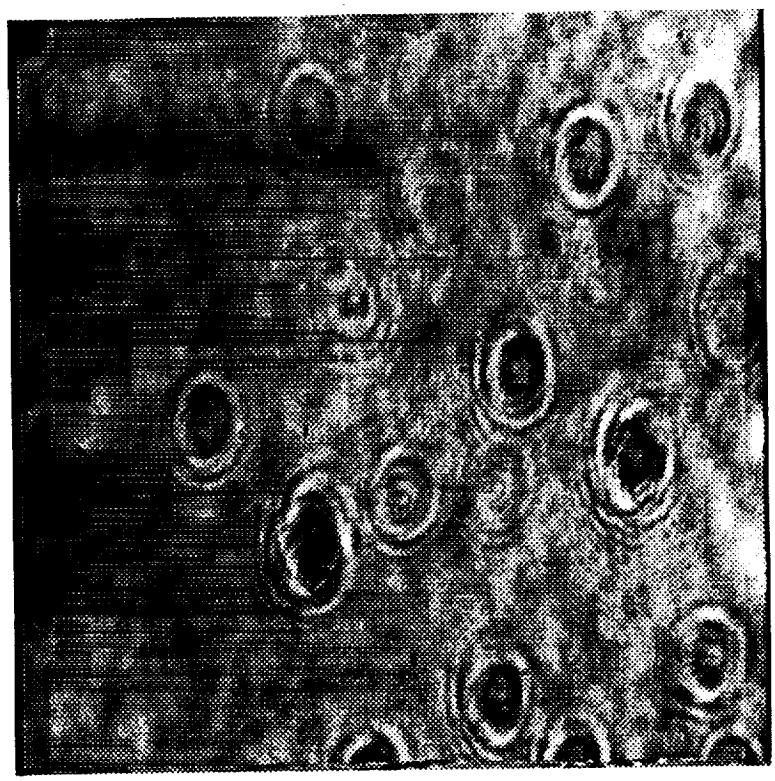

Figure 3: Successive raw image of diffraction patterns of 5 μm alumina particle in water.

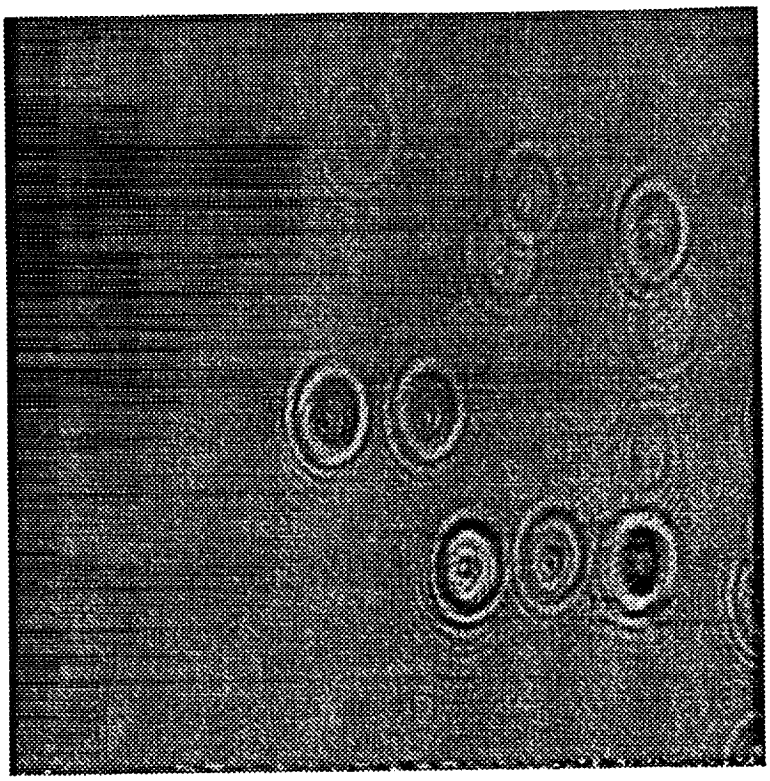

Figure 4: Subtraction of images shown in Fig.s 2 and 3 to eliminate optical noise due to dust and laser speckle.

enhancement technique is used to make the rings more visible. Ring visibility is essential, since the size of the rings gives information regarding the location of the particle relative to the focal plane of the lens as well as makes the task of finding the centroid of the particle much simpler.

An even better example of how image processing can be used to improve fringe visibility is shown in Fig. 7. A much poorer raw image of particles much closer to the imaging plane is shown (obtained for different lighting conditions). The particles are visible in this figure, but the fringe patterns are not well-defined. Application of a sobel-abs filter makes the fringes visible as is obvious in Fig. 8. A subsequent contrast enhancement is used to create a nearly binary image makes the fringes even more visible, as is seen in Fig. 9.

As the optics and lighting requirements have been ironed out, a calibration rig has been designed and constructed for the purpose of proving the accuracy of the 3-D P.I.V. technique in the range of velocities expected in the future flight experiment ($< 10\mu$m /sec). It consists of a rectangular channel 1 mm by 10 mm in cross-section, which will provide a known Poiseuille velocity distribution, to which the 3-D P.I.V.

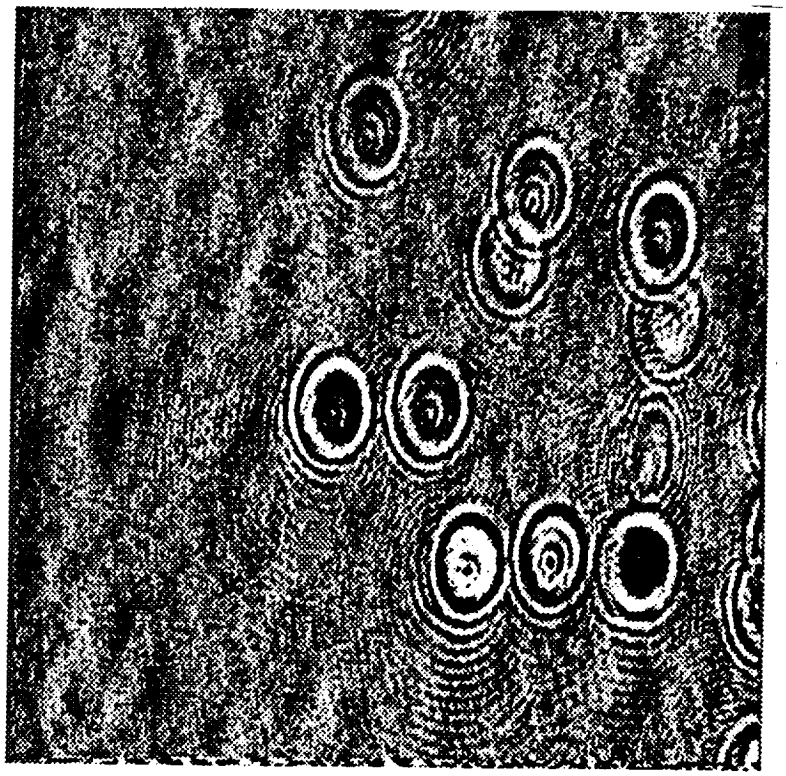

Figure 5: Enhancement contrast of image shown in Fig. 4 to improve the fringe visibility.

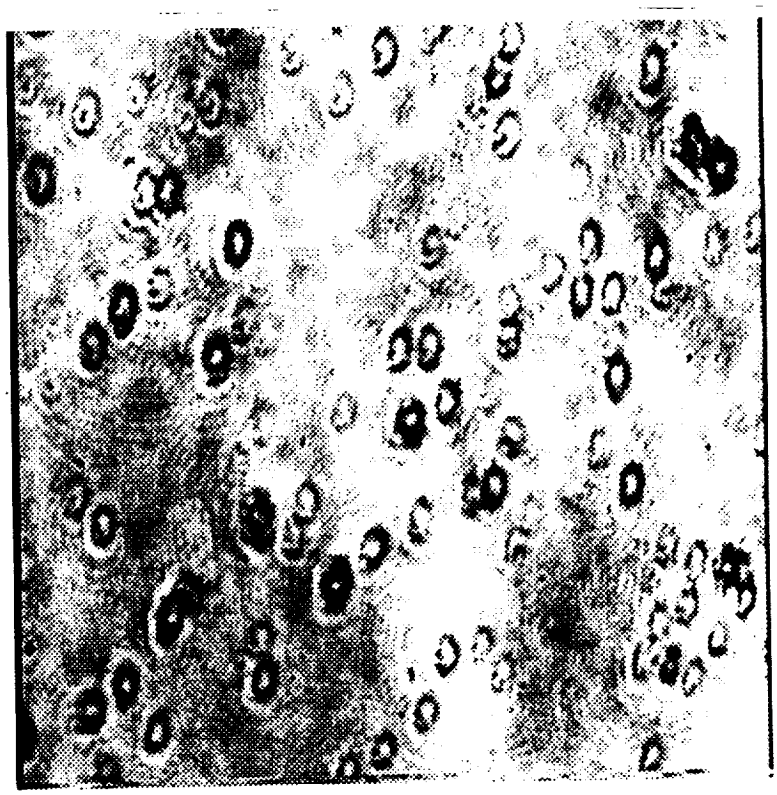

Figure 6: Raw image of particles (5 micron alumina in water) with much poorer visibility.

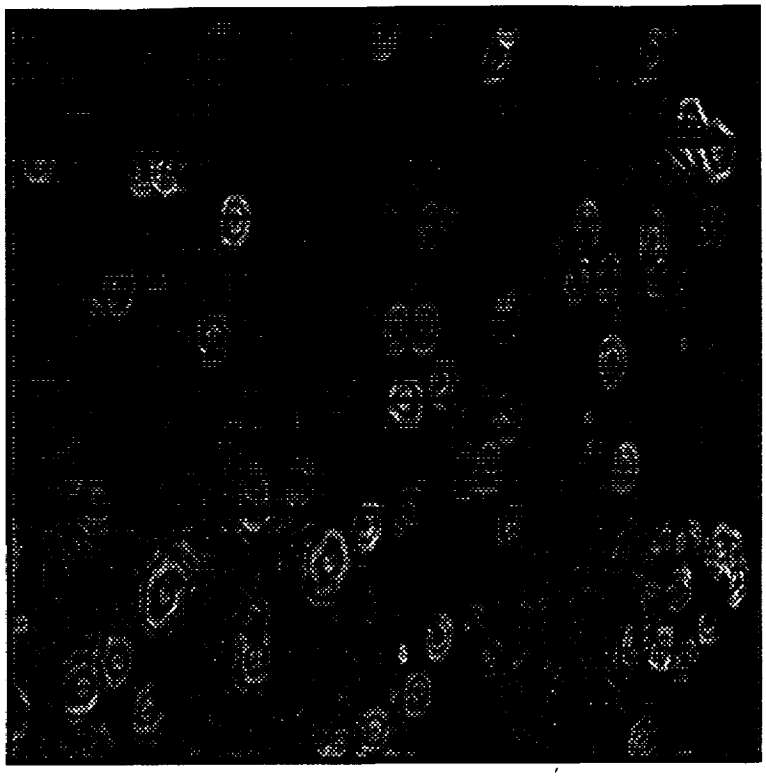

Figure 7: Sobel-abs filter on raw image shown in Fig. 6.

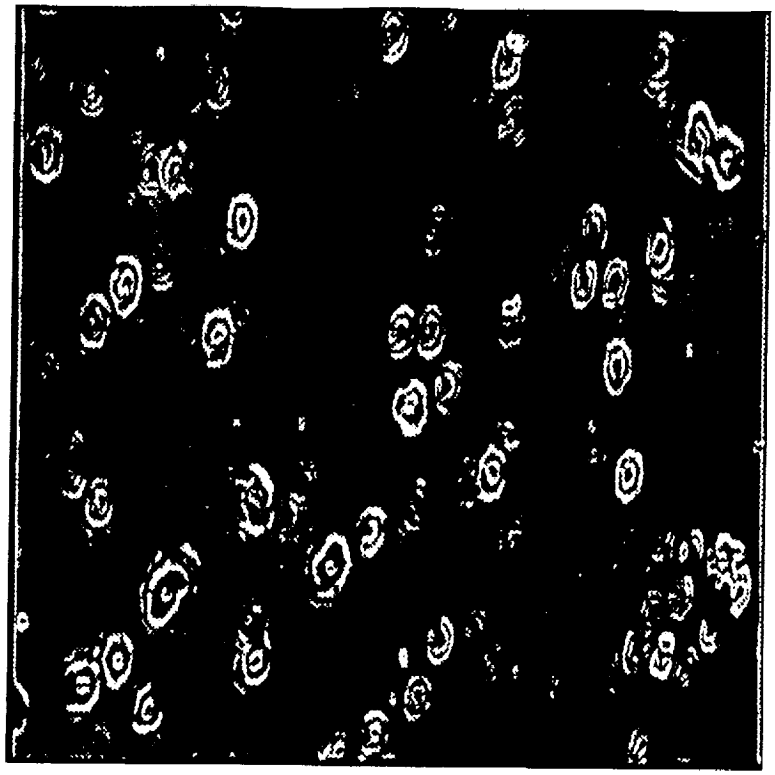

Figure 8: Contrast enhancement of Fig. 7.

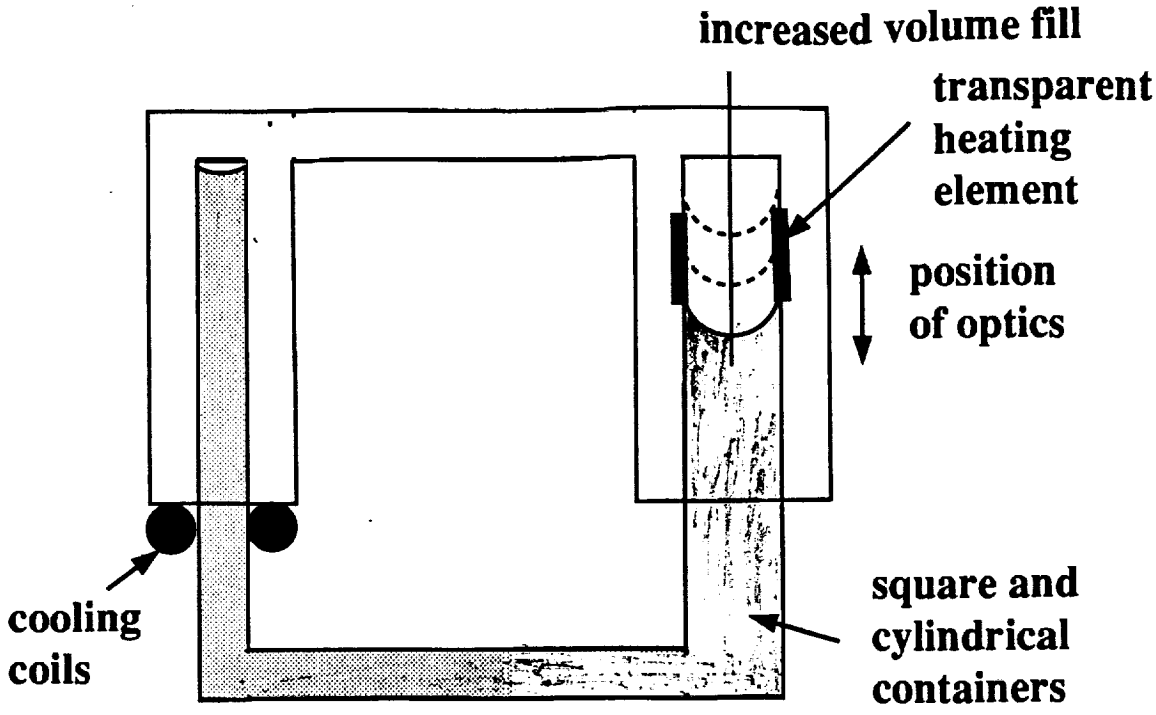

Figure 9: Calibration rig for 3-D P.I.V.

velocity measurements can be compared. This facility is ready for use, but is currently being modified to allow for the use of a syringe pump to force the liquid through the test cell at a known velocity. A schematic of the test cell is shown in Fig. 8.

Students

1. Qun He - Mechanical Engineering Ph. D. student. Since Jan. 1, 1993. Primarily involved in experimental development.

2. Kamal Das - Electro-Optics Ph.D student. Since Sept. 1, 1993. Will be working closely with Ben Ovryn to develop theoretical basis for technique.

Numerical Modelling of the Thin Evaporating Film

A model of the thermo-fluid behavior of the thin evaporating thin film adjoining the bulk capillary meniscus, where evaporation is affected by heating at the outside wall of the capillary, has been developed for 0-g, with particular emphasis on the large tube sizes to be considered in the 0-g testing. This model has been developed to obtain an estimate of the heating conditions which can be tolerated in 0-g before the onset of thermocapillary flows on the non-isothermal liquid-vapor interface. The space tests are designed to

study only a stable evaporating meniscus and only the conditions present at the onset of an instability are of interest. As well, the model has been developed to gauge the required accuracies for measurement of the thin film velocity field, film thickness, power input, and wall and possibly interfacial temperature measurement.

Appendix A shows results from the modeling efforts of the the steady evaporation from the thin film region of the meniscus for varying pore sizes and considering pentane as the working fluid. Pore diameters of 10μm, 1 mm, and 10 cm were considered. Additionally, for each of these pore sizes different heating rates as expressed through the difference between the wall temperature and the vapor temperature, $T_w - T_v$ were considered. The basic aim of this initial work was to primarily get the numerical solution of the model working. Now, that it is working, future work will concentrate on realizing the goals described in the previous paragraph.

Students

1. Houssam Chebaro - Mech. Eng. Post-doctoral student. Jan. - Feb., 1993.
2. Qun He- Mech. Eng. Ph.D. student. Since Jan. 1, 1993.

Publication/Conference Presentation

1. H.C. Chebaro and K. P. Hallinan, "Boundary Conditions for an Evaporating Thin Film for Isothermal Interfacial Conditions," J. Heat Transfer, 115, pp. 816-819.
2. H. C. Chebaro, K. P. Hallinan, S. J. Kim and W. S. Chang, "Evaporation from a Porous Wick Heat Pipe for Non-Isothermal Conditions," presented at Nat.l Heat Transfer Conference, Atlanta, Georgia, Aug. 8-11, 1993. Also in submission.

Conceptualization of Space Flight Test Loop

The third task has focused on the space flight test cell configuration. It has aimed at: (i) providing a means for filling the cell in flight, and (ii) providing a passive means for control of the evaporating meniscus location. Initially the test cell or loop was envisioned to be comprised of parallel evaporator and condenser 'legs'. The evaporator leg was envisioned to be a square cuvette (both inside and outside), having optically flat inner and outer surfaces. However, subsequent drop tower testing of an evaporating meniscus within a

square cuvette revealed that the corners, as expected, effectively wicked the bulk liquid within the cuvette up the corners of the tube. Initially, it was proposed to use barrier coatings within the corners to prevent this. However, subsequent investigation showed that it would be very difficult to preferentially apply the barrier coatings only in the corners. Also it was determined that it would be very difficult to heat the meniscus uniformly about the periphery of the evaporator meniscus, and thus the square geometry would be prone to perimeter thermocapillary flows. So at the cost of slight curvature for the large tube sizes of interest in the space experiment, a circular tube was selected for use in all future considerations.

The final configuration of the loop was envisioned to consist of parallel evaporator and condenser legs which are connected at top and bottom. The loop would be filled from the bottom with liquid. The condenser leg would be of a smaller diameter than the evaporator leg to insure that the entering liquid to the loop first wicks to the top of the condenser leg, which will intersect a porous copper felt, to be used to 'spread out the condenser area', before it fills the evaporator leg. Once the liquid has wicked to the top of the porous felt, any subsequent fill into the loop will cause the evaporator tube to fill. The volume fill of liquid into the loop will thus control the meniscus location within the evaporator. The design concept is shown schematically in Fig. 11.

Students

1. Paul Beer, Ray Simon - Mech. Eng. undergraduates - winter 1993.
2. Ilya Lisenker - Mech. Eng. undergraduates - May 1993 -present.
3. Ray Simon - Mech. Eng. M.S. student funded through U.D. - May 1993 -present.
4. David Pratt - Mech. Eng. Ph.D. student, Air Force - May 1993 - present.

Prototype Construction of Test Cell Loop(s)

Several test cell loops were constructed. One was constructed just to proove that the filling technique described above could be used to control the location of the evaporator meniscus relative to the end of the evaporator tube, and therefore relative to the location of gold film heating element(s) vapor deposited on the outside of the evaporator tube. Two others were constructed for the purpose of both 1-g testing and for serving as a prototype for 0-g tests to be performed in the drop-towers or perhaps the aircraft in the winter

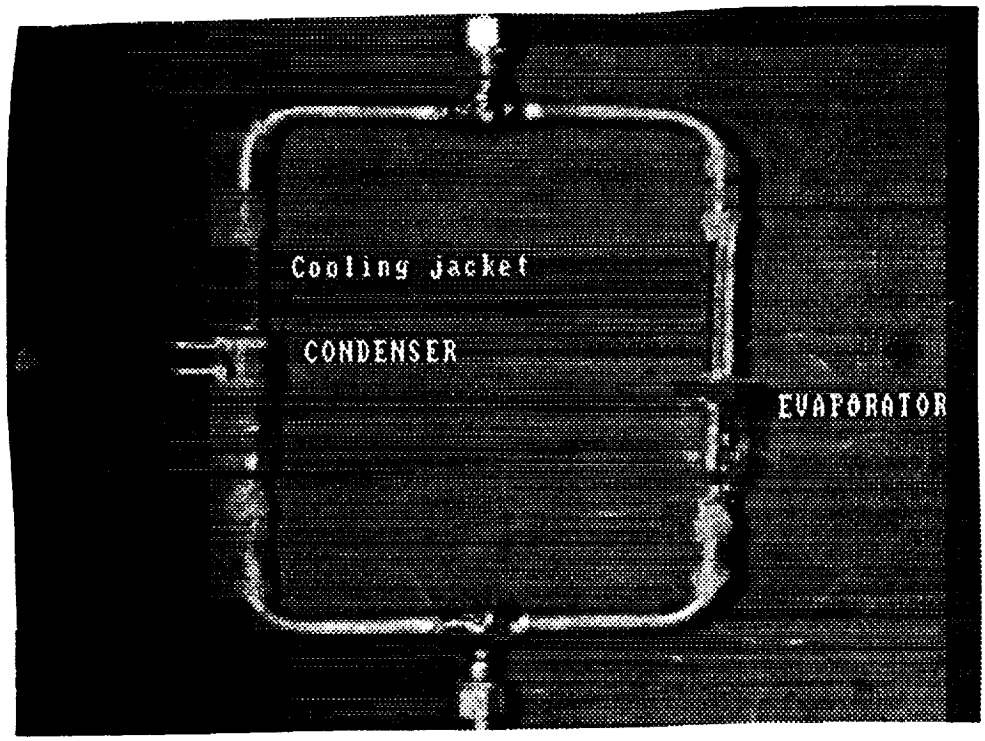

Figure 10: Preliminary test loop for evaluating concept for filling the loop in-flight and for controlling the meniscus location.

of 1994 through the summer of 1994. These loops have been configured and preliminary experiments have been conducted.

The preliminary test loop has been constructed according to Fig. 11 to verify that this design is adequate for ease of filling in flight as well as for controlling the location of the meniscus in the evaporator tube. The tube sizes for the preliminary design were 0.5 and 3 mm, respectively for the condenser and evaporator tubes. Small tube sizes were used to approximate the conditions which would be present in the big tubes which will be used in the space microgravity testing. The design has been shown to be successful on both accounts.

The 1-g test loop is configured as shown in Fig. 12. In it, a capillary tube is vertically oriented in bath of liquid (pentane) in a beaker. Gold film heating element(s) are vapor deposited to the outside diameter of the capillary tubes, each approximately 1 cm in length. (See Fig. 13 for details of the gold films). The level of the reservoir relative to the top end of the capillary tube is variable to allow for the possibility of pinning the meniscus at the top of the capillary tube. The reservoir is cooled by circulating a variable temperature cooling fluid through a copper tube heat exchanger which is immersed in the liquid reservoir. The test configuration is located within a bell jar with multiple ports for visual observation of the meniscus. The evaporating meniscus within the capillary tube is observed using a long-distance microscope.

In the preparation of this rig a number of supporting activities had to be refined and perfected. Cleaning procedures for glassware and tubing were perfected, so that now reproducibly 'clean' cells can be obtained. Vapor deposition techniques for the gold film have been experimented with to insure a uniform thickness gold film. Calibration devices for the gold film as well as thermocouples have been perfected to insure uncertainties for each less than $\pm 0.1°C$ for each. Also experience with the gold film has shown that annealing of the gold film is necessary to insure that the gold film resistance remains constant with time. This set-up is ready for testing.

The experiment is to be conducted to simulate the experiments which will be consducted in microgravity in much larger tube sizes, where effectively the Bond numbers associated with both the capillary tube and the evaporator tube are small, such that gravity effects are negligible. Thus the bulk liquid motion and the stability of the evaporating meniscus can be observed as a function of heat rate, evaporator tube size, and proximity of the meniscus relative to the end of the tube. These observations will provide more useful knowledge which will aid in the configuration of the ultimate space flight experiments.

The additional loop, shown schematically in Fig. 14, is being configured to serve as a model for the

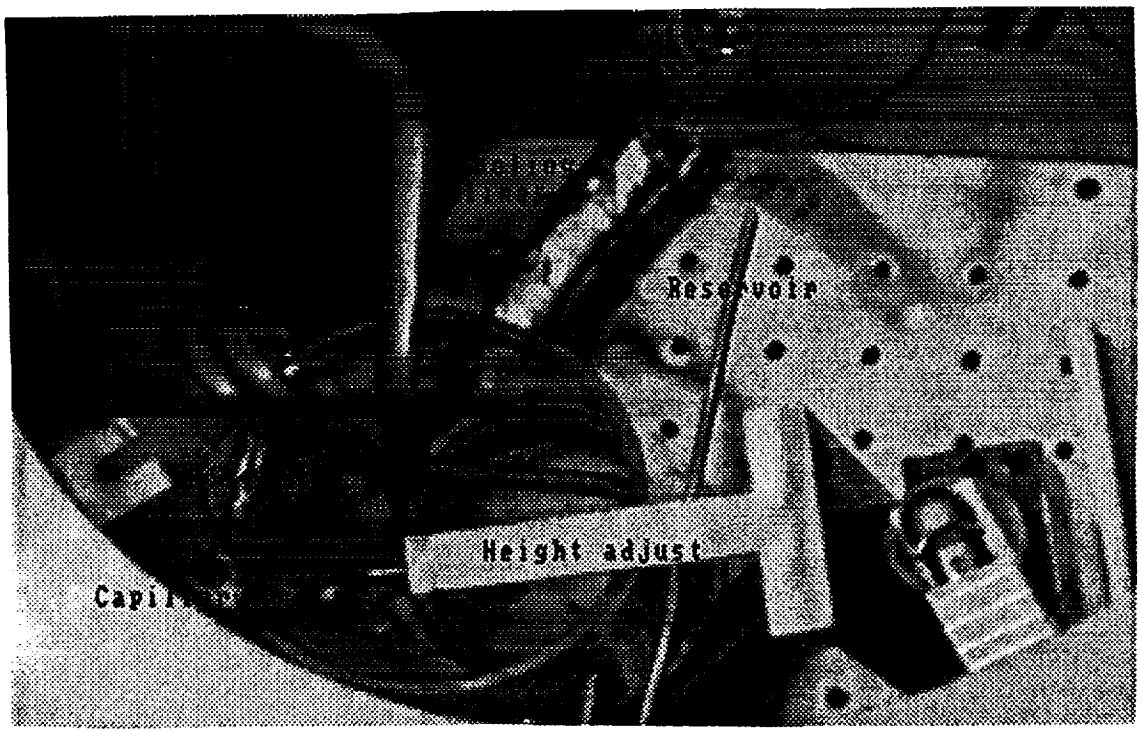

Figure 11: Test rig for testing evaporation from a capillary meniscus in 1-g at low Bond numbers

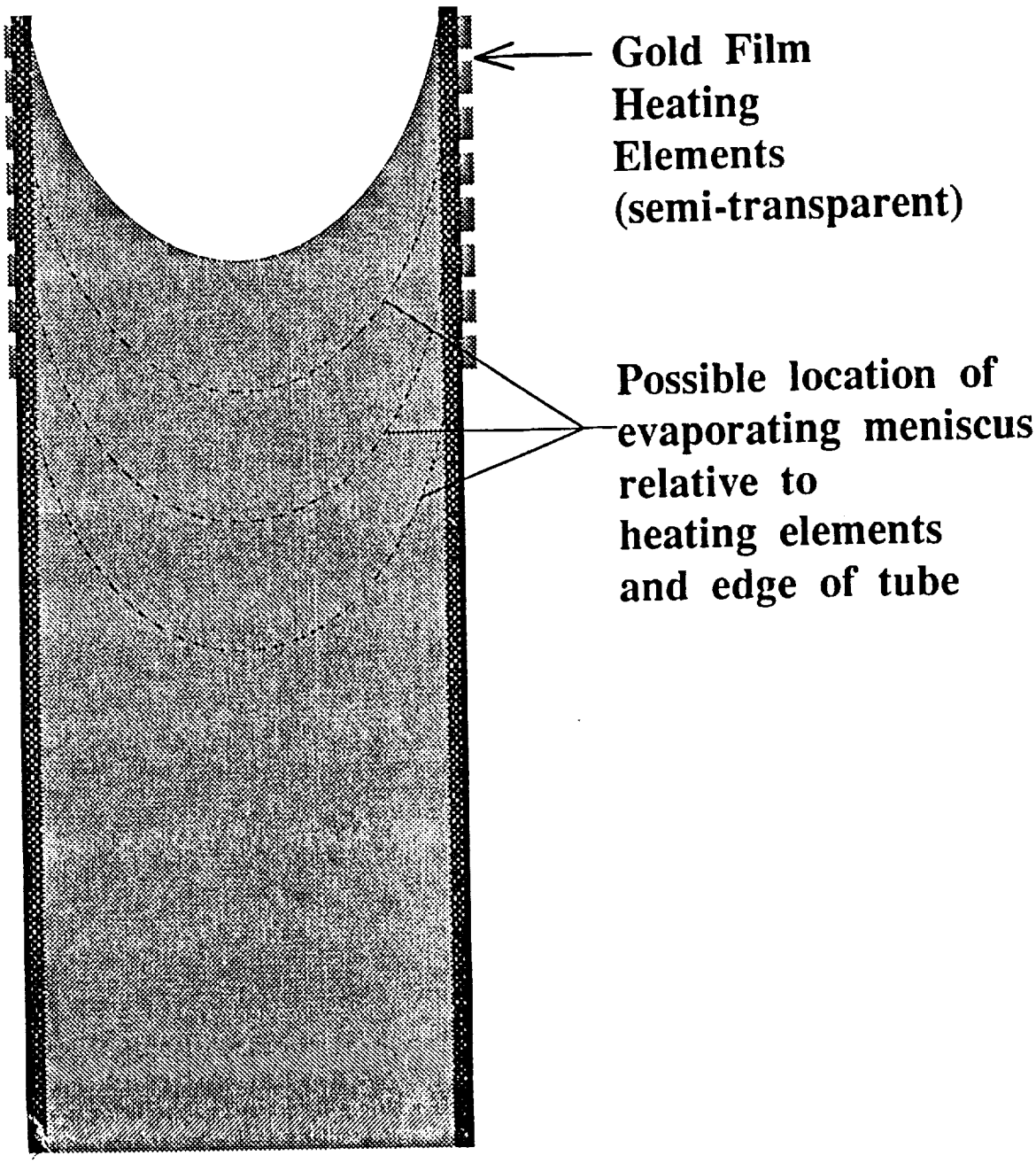

Figure 12: Schematic of circumferential gold film heating elements

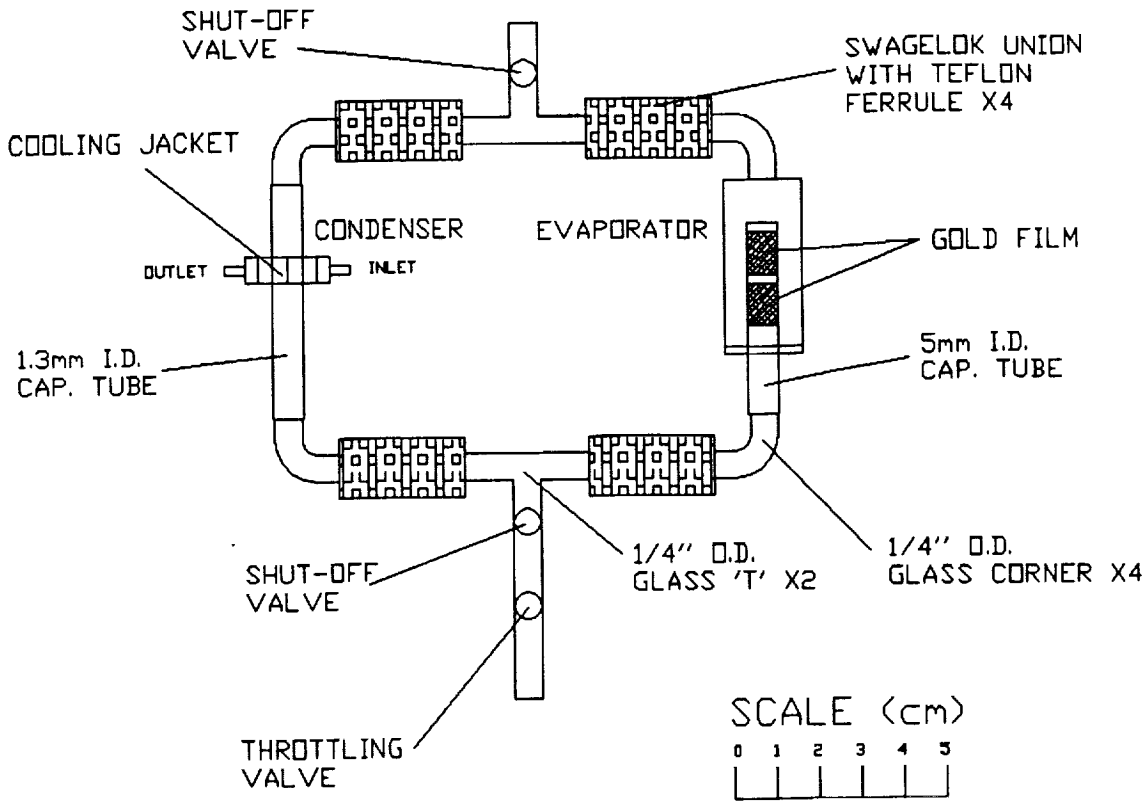

Figure 13: Test loop which will serve as a model for the construct of test loops to be operated in earth-based low gravity testing

fabrication at NASA-LeRC of a test loop to be used in testing in the ground-based low-g testing environments available at NASA-LeRC. It will be helpful in evaluating the soundness of the design for the loop in these tests.

Students

1. Ilya Lisenker - Mech. Eng. undergraduate- May 1993 - present.

2. Ray Simon - Mech. Eng. M.S. student - May 1993 - present.

3. David Pratt - Mech. Eng. Ph.D. student - May 1993 -present.

Zero-g Drop Tower Testing

A drop tower rig was configured at NASA-LeRC for the 2.2 second drop tower to study evaporation from a meniscus of acetone within a square cuvette via depressurization of the vapor above the meniscus. The goals of the experiment were primarily to: (i) gain insight into the process of evaporation from a capillary meniscus in a low gravity environment; (ii) assess the appropriateness of a square cuvette for serving as the capillary in the future flight experiments; and (iii) qualitatively observe the importance of thermocapillary flows via tracking of particles seeded in the flow for increasing total evaporation rates.

Experiments were then conducted during the summer of 1993. The square tube was observed to clearly be inappropriate for further consideration as the liquid within the tube would wick up the corners of the tube very rapidly. Thus control of the meniscus location in a square tube would be very difficult. Thermocapillary flows were observed as the total evaporation rate was increased, i.e., the vapor pressure was reduced. However, extrapolation to the conditions which will be present in the desired loop, where wall heating will be used to affect evaporation, is not possible. One trend was apparent though. In 1-g the bulk flows which were present within the cuvette for similar conditions in 0-g were far more severe. Given the aspect ratios in the loop (height of liquid column to width of test cell) buoyancy was clearly the dominant mechanism for flow in the cell for the 1-g tests.

Student

1. Jeffrey Allen - Mech. Eng. Ph.D. student - Dec. 1993 - present.

Effect of Vibrations on Evaporating Meniscus

The final task, only recently begun, has aimed at quantifying the effect of vibrations on the meniscus stability for both evaporating and non-evaporating conditions within both single circular tubes and for the proposed loop configuration. Both slosh mode and natural frequency mode disturbances are being studied experimentally now in 1-g. The effects of varying frequency, amplitude, orientation, test cell size, fluid, and proximity of the meniscus to the edge of a tube are being investigated on the stability of the meniscus for both geometries. A shaker table is being used to provide the oscilations.

After completion of the 1-g studies it is desired to perform similar experiments in a 0-g environment.

Student

1. David Valociek - Mech. Eng. M.S. student, NASA -GSRP fellow - July 1993 - present.

Appendix A

NUMERICAL ANALYSIS RESULTS

FOR THIN FILM REGION OF HEAT PIPE

A. Small Pore (Diameter is 10 micron)

(1). Effects of Different Tw-Tv.

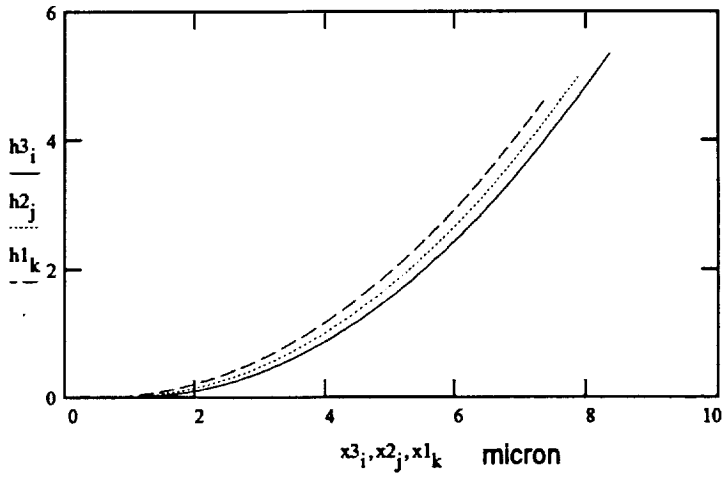

Thickness (micron) of Thin Film for different Tw-Tv

Tw-Tv= 0.002C(for h3), 0.02C(for h2), 0.05C(for h1)

Pentane, Diameter of the pore is 10 micron (Ma=0)

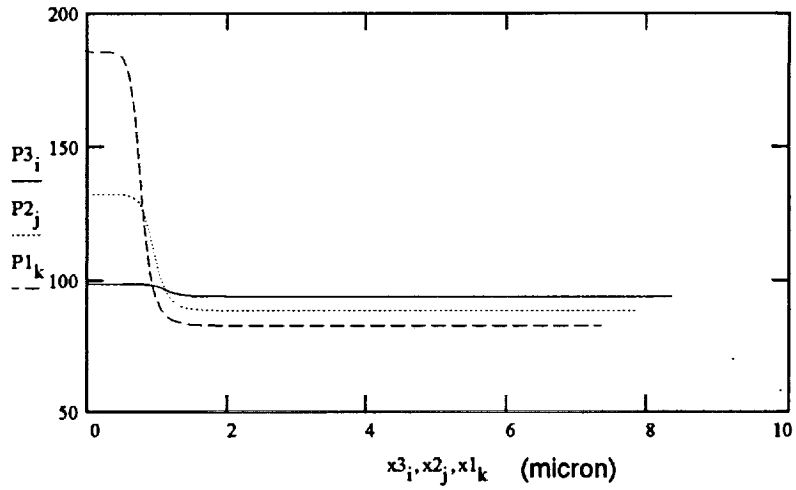

Pressure (kPa) of Thin Film for different Tw-Tv

Tw-Tv=0.002C(for P3), 0.02C(for P2), 0.05C(forP1)

Pentane, Diameter of the pore is 10 micron (Ma=0)

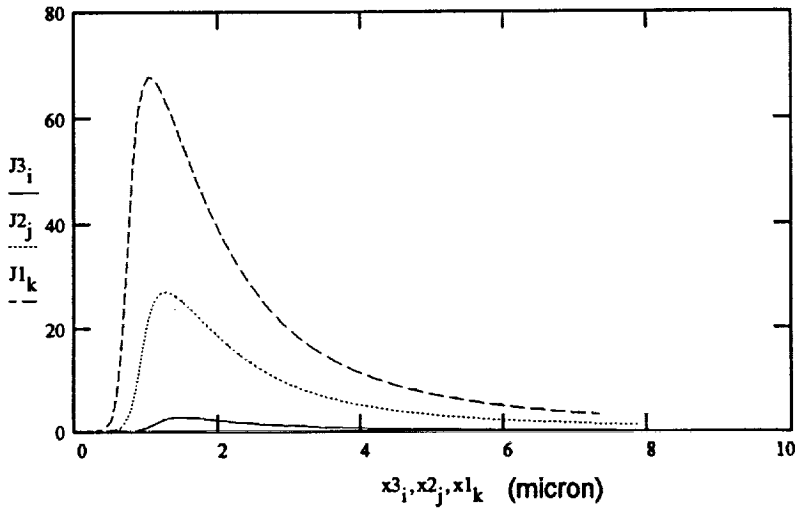

Mass Flux (g/m^2s) of Thin Film for different Tw-Tv

Tw-Tv= 0.002C(for J3), 0.02C(for J2), 0.05C(for J1)

Pentane, Diameter of the pore is 10 micron (Ma=0)

(2) Effects of Marangoni Number

Tw-Tv=0.002c

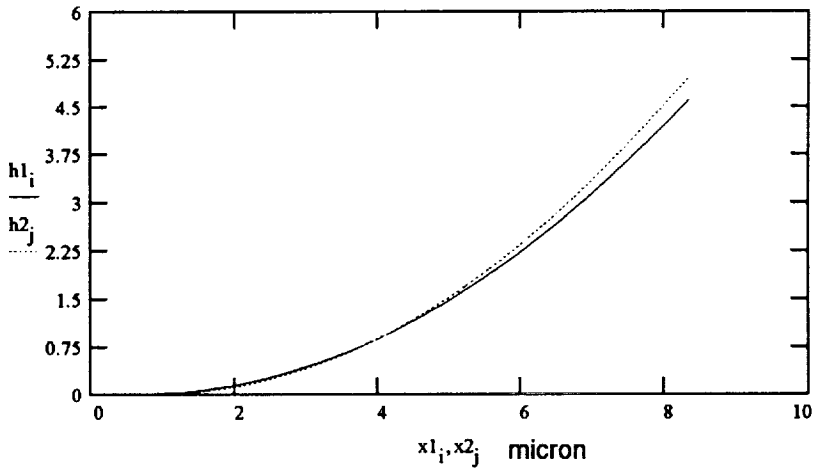

Effect of Marangoni number

Thin film thickness (micron) h1(Ma=0), h2(Ma=2.502e-6)

Tw-Tv=0.002C, Pentane, Size of pore is 10 micron

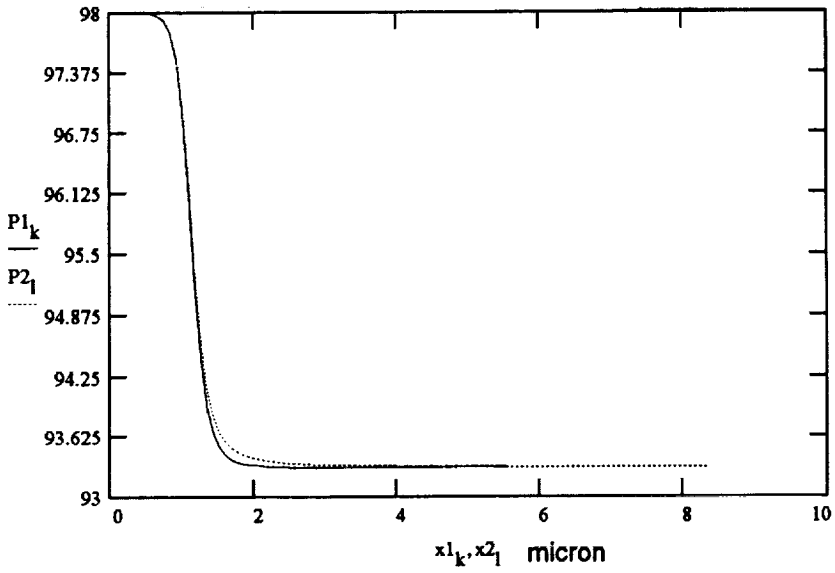

Effect of Marangoni number

Thin film Pressure (kPa) P1(Ma=0), P2(Ma=2.502e-6)

Tw-Tv=0.002C, Pentane, Size of pore is 10micron

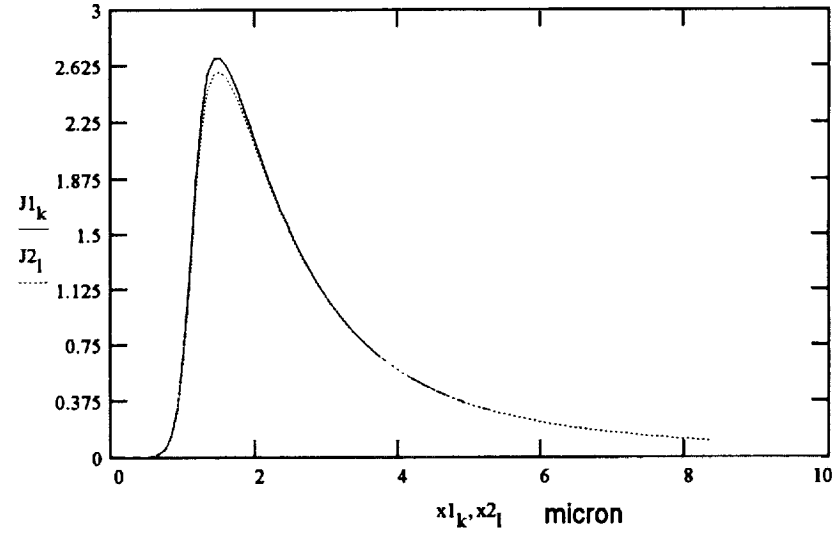

Effect of Marangoni number

Thin film Mass Flux (g/m^2s) J1(Ma=0), J2(Ma=2.502e-6)

Tw-Tv=0.002C, Pentane, Size of pore is 10 micron

Tw-Tv=0.05c

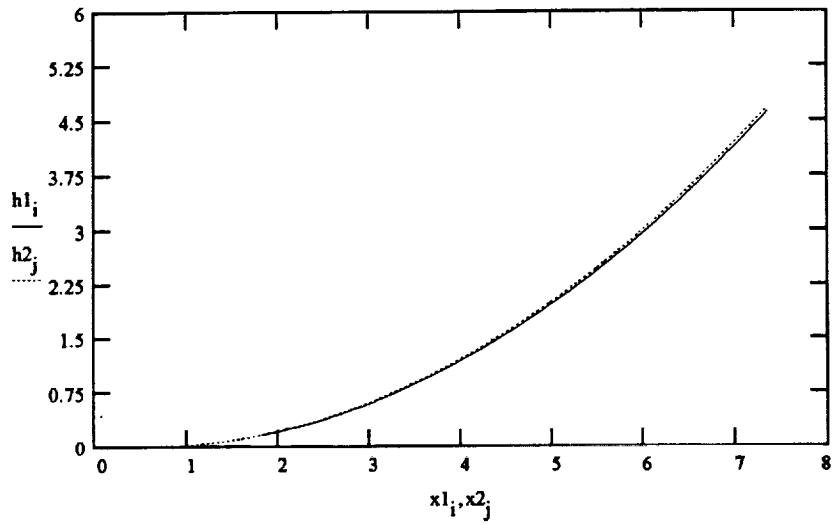

Effect of Marangoni number

Thin film thickness (micron) h1(Ma=0), h2(Ma=4.265e-5)

Tw-Tv=0.05C, Pentane, Size of pore is 10 micron

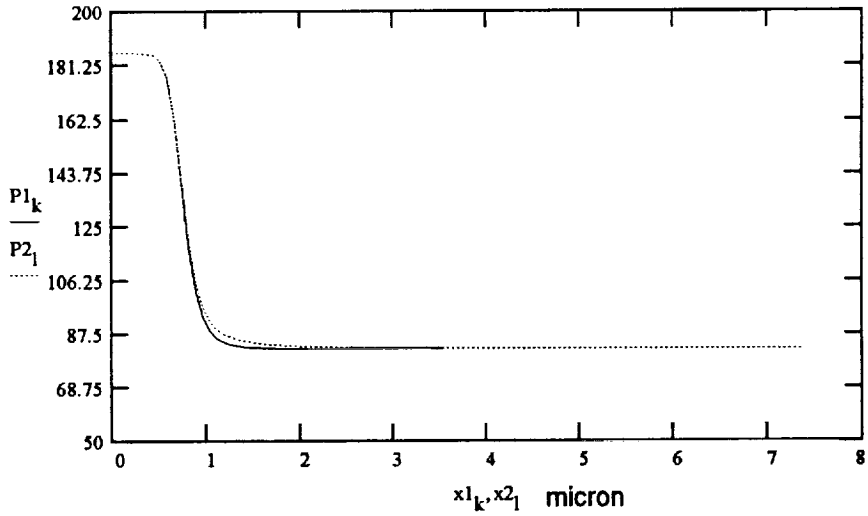

Effect of Marangoni number

Thin film Pressure (kPa) P1(Ma=0), P2(Ma=4.265e-5)

Tw-Tv=0.05c, Pentane, Size of pore is 10 micron

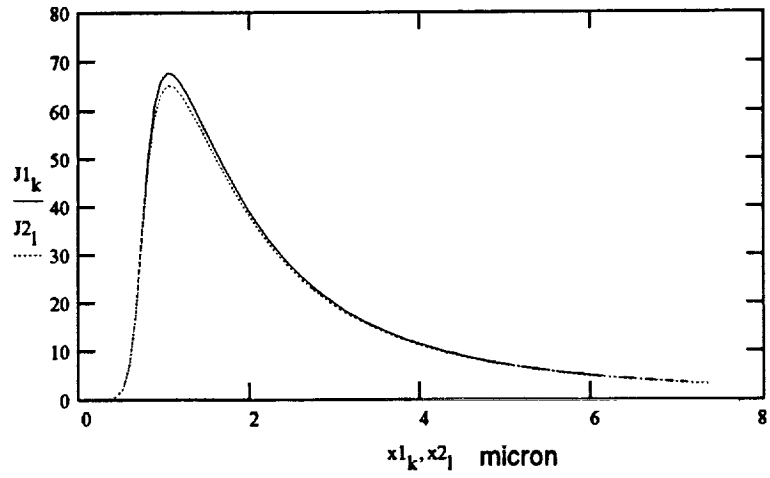

Effect of Marangoni number

Thin film Mass Flux (g/m^2s) J1(Ma=0), J2(Ma=4.265e-5)

Tw-Tv=0.05c, Pentane, Size of pore is 10 micron

B. Middle Pore (Diameter is 1 mm)

(1) Effects of Different Tw-Tv

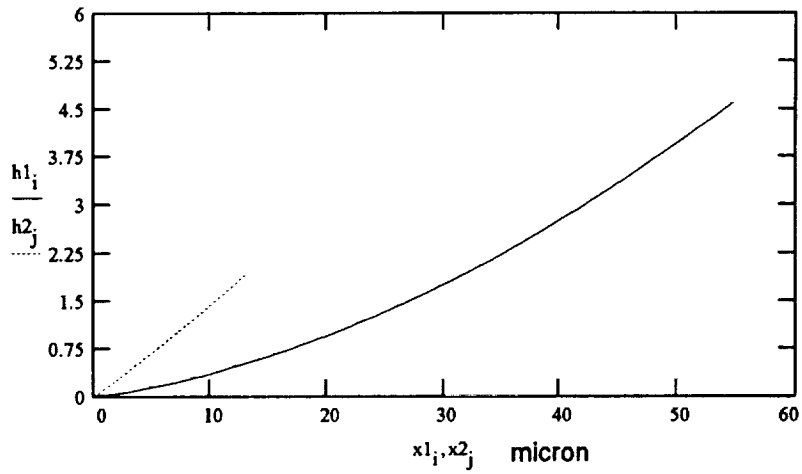

Effect of different Tw-Tv

Thin film thickness (micron) h1(Tw-Tv=0.002c), h2(Tw-Tv=0.02

Ma=0, Pentane, Size of pore is 1mm.

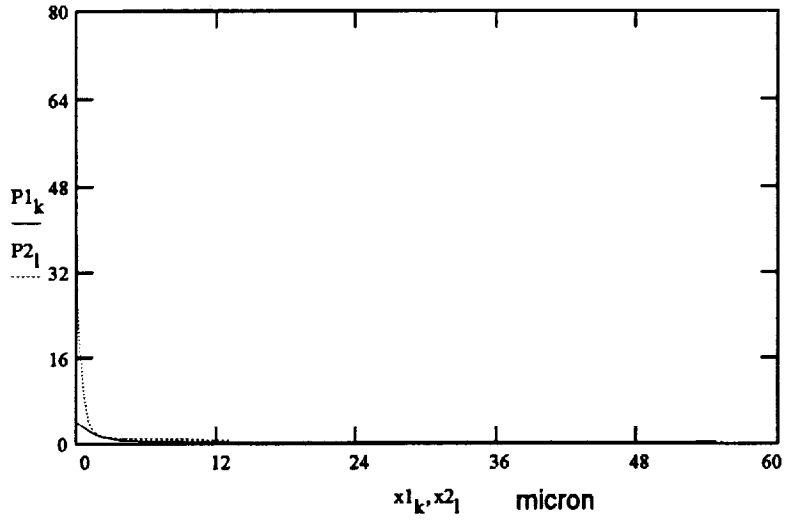

Effect of different Tw-Tv

Thin film Pressure (kPa), P1(Tw-Tv=0.002c), P2(Tw-Tv=0.02c)

Ma=0, Pentane, Size of pore is 1mm.

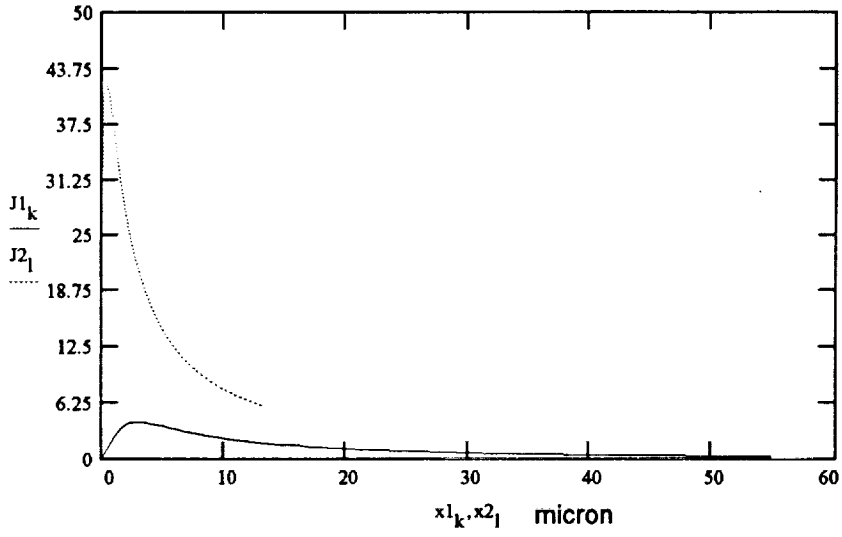

Effect of different Tw-Tv

Thin film Mass Flux (g/m^2s), J1(Tw-Tv=0.002c), J2(Tw-Tv=0.02

Ma=0, Pentane, Size of pore is 1mm.

(2) Effects of Marangoni Number

Tw-Tv=0.002c

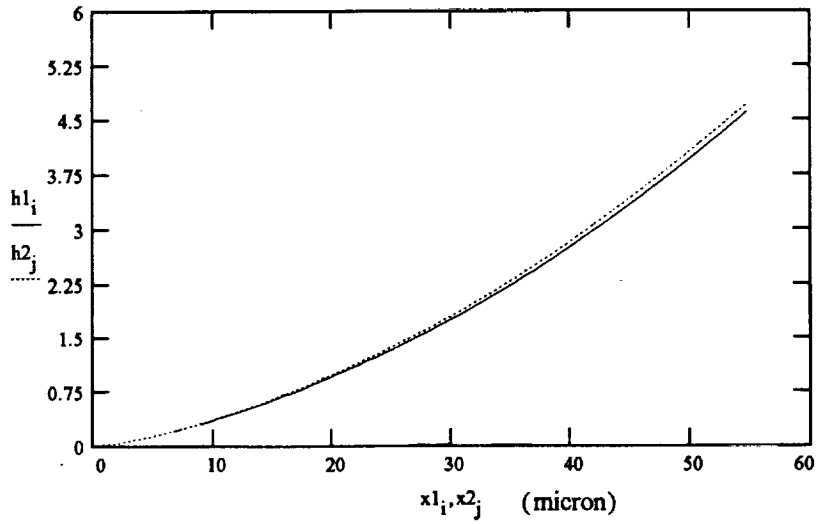

Effect of Marangoni number

Thin film thickness (micron) h1(Ma=0), h2(Ma=2.564e-6)

Tw-Tv=0.002C, Pentane, Size of pore is 1mm

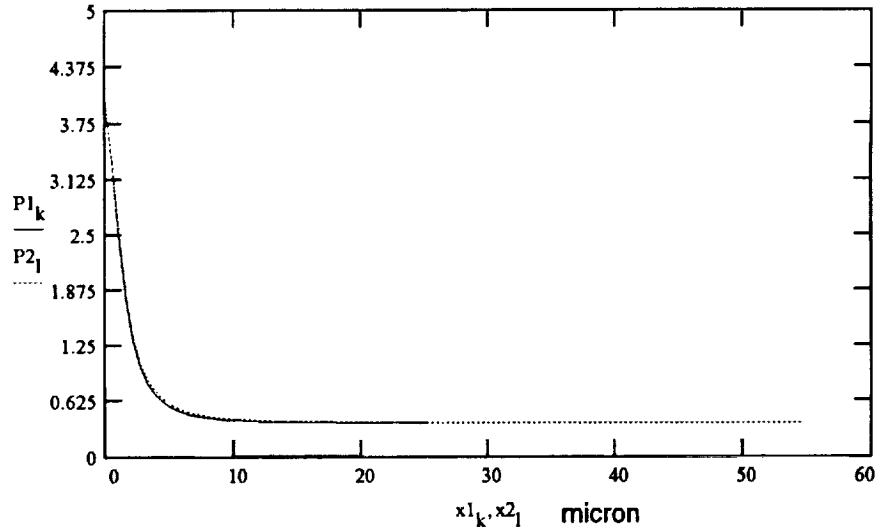

Effect of Marangoni number

Thin film Pressure (kPa) P1(Ma=0), P2(Ma=2.564e-6)

Tw-Tv=0.002C, Pentane, Size of pore is 1mm

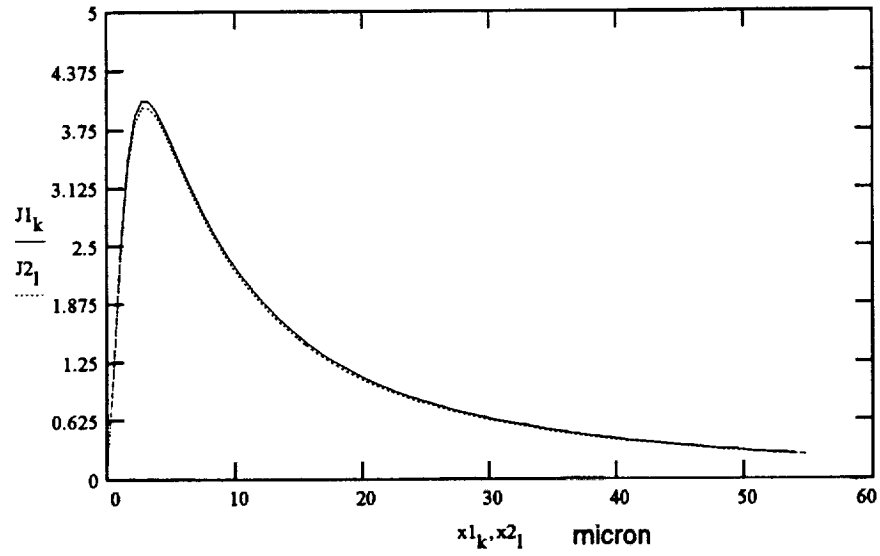

Effect of Marangoni number

Thin film Mass Flux (g/m^2s) J1(Ma=0), J2(Ma=2.564e-6)

Tw-Tv=0.002C, Pentane, Size of pore is 1mm

C. Large Pore (Diameter is 10 cm)

(1) Effects of Different Tw-Tv (Marangoni numbers are not zero)

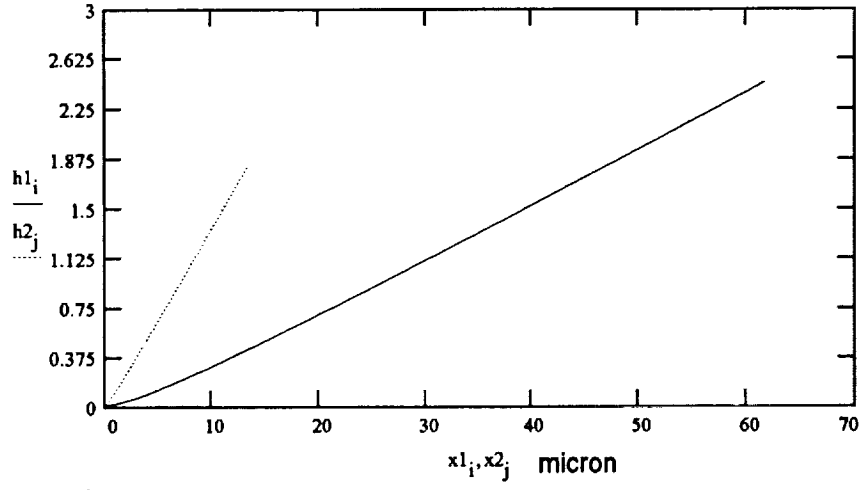

Thin film Thickness (micron), (Pentane, Size of pore is 10cm)

h1 (Tw-Tv=0.002c, Ma1=2.564e-6), h2 (Tw-Tv=0.02c, Ma2=2.564e

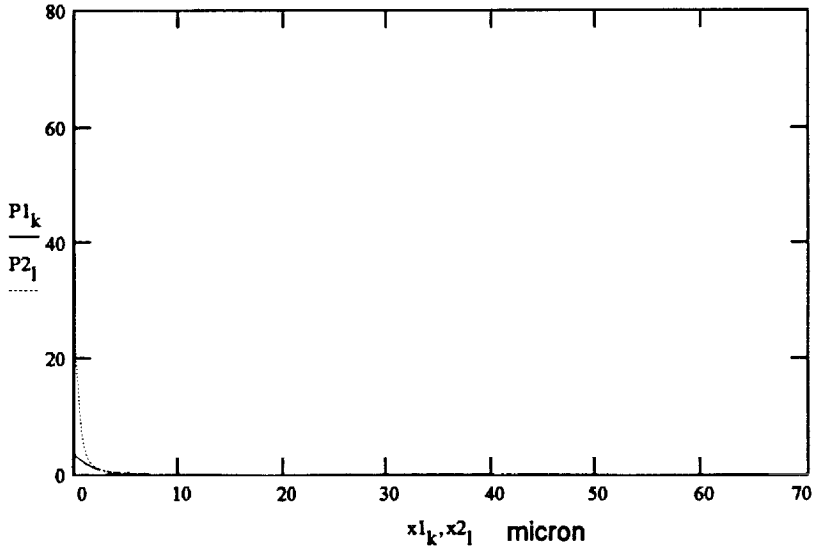

Thin film Pressure (kPa), (Pentane, Size of pore is 10cm)
P1 (Tw-Tv=0.002c, Ma1=2.564e-6), P2 (Tw-Tv=0.02c, Ma2=2.564e-

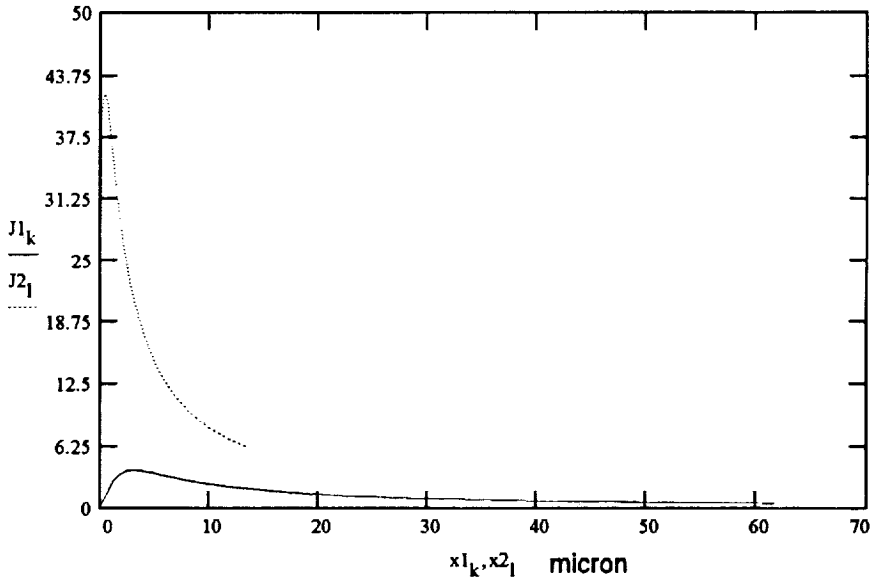

Thin film Mass Flux (g/m^2s), (Pentane, Size of pore is 10cm)
J1 (Tw-Tv=0.002c, Ma1=2.564e-6), J2 (Tw-Tv=0.02c, Ma2=2.564e-

(2) Effects of Marangoni Numbers

Tw-Tv=0.002c

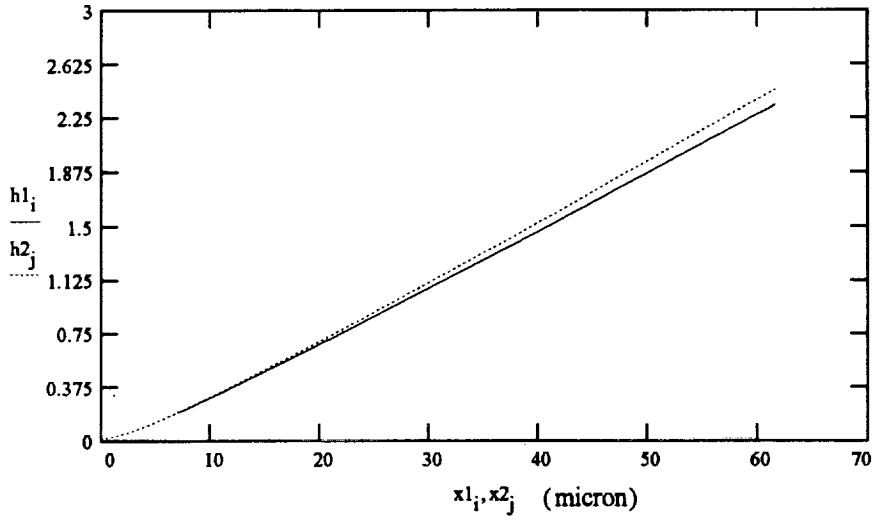

Effect of Marangoni number

Thin film thickness (micron) h1(Ma=0), h2(Ma=2.564e-6)

Tw-Tv=0.002C, Pentane, Size of pore is 10cm

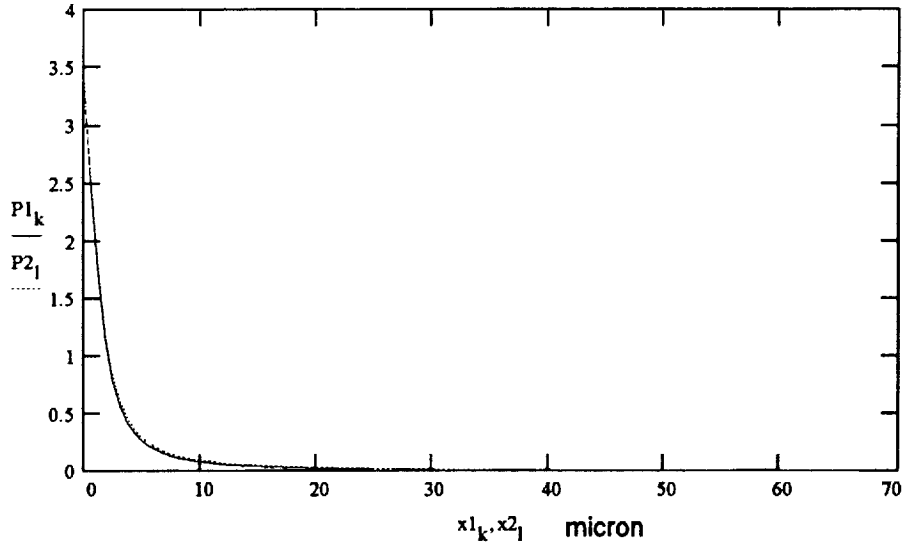

Effect of Marangoni number

Thin film Pressure (kPa) P1(Ma=0), P2(Ma=2.564e-6)

Tw-Tv=0.002C, Pentane, Size of pore is 10cm

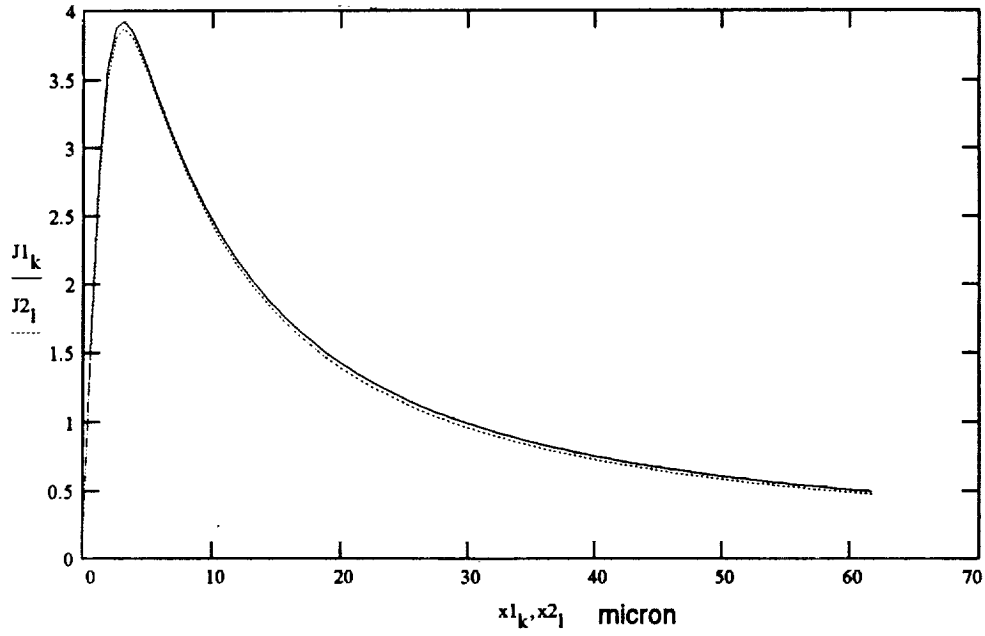

Effect of Marangoni number

Thin film Mass Flux (g/m^2s) J1(Ma=0), J2(Ma=2.564e-6)

Tw-Tv=0.002C, Pentane, Size of pore is 10cm